Reprinted from The Journal of Physical Chemistry, 1993, 97.

Global Energy Minimum Searches Using an Approximate Solution of the Imaginary Time Schrödinger Equation

Patricia Amara, D. Hsu,† and John E. Straub*

Department of Chemistry, Boston University, Boston, Massachusetts 02215

Received: February 3, 1993

We present a method for finding the global energy minimum of a multidimensional potential energy surface through an approximate solution of the Schrödinger equation in imaginary time. The wave function of each particle is represented as a single Gaussian wave packet, while that for the n-body system is expressed as a Hartree product of single particle wave functions. Equations of motion are derived for each Gaussian wave packet's center and width. While evolving in time the wave packet tunnels through barriers seeking out the global minimum of the potential energy surface. The classical minimum is then found by setting Planck's constant equal to zero. We apply our method first to the pedagogically interesting case of an asymmetric double-well potential and then use it to find the correct global energy minima for a series of Lennard-Jones n-mer clusters ranging from $n = 2$ to 19.

I. Introduction

In recent years a picture of disordered systems has emerged which describes structure and dynamics in terms of a multidimensional potential hypersurface. The potential hypersurface consists of many attractive basins or minima with a distribution of relative energies. Each basin is characterized by a volume and the energy of its minimum. This model has been applied to liquids and glasses as the "inherent structure model" of Stillinger and Weber[1] and to proteins as the "conformational substates model" of Frauenfelder and co-workers.[2] Formally, the configurational integral of the system can be expressed in terms of separate integrals over the various attractive basins. To determine the equilibrium properties of the system, a good approximation may be to enumerate these minima, weight them by their relative energies (and entropies), and average over them.[3] Additionally, with a knowledge of the connectivity of the attractive basins and the distribution of barrier heights which must be crossed to move from one basin to another, dynamical properties may also be accessed.[4]

In problems such as protein folding, one expects only one or a few important energy minima (or classes of minima) to dominate the thermodynamics because the specificity of protein function depends on the uniqueness of its natural structure. In such a picture, a protein's folded structure can be determined by finding the compact state of lowest free energy for the protein–solvent system. That is, the protein folding problem can be reduced to finding the global minimum of the many-dimensional free energy hypersurface. This is essentially a static approach to the protein folding problem as opposed to the kinetic approach of letting the protein fold through straightforward molecular dynamics. A problem with the dynamic approach is that at the moment the time scale for kinetic protein folding for most proteins is well beyond that attainable on the fastest computers.

A wide variety of energy minimization methods have been proposed with an eye on solving the static problem. Many of them have been developed by Scheraga and co-workers.[5] In a recent advance, Piela, Kostrowicki, and Scheraga have proposed the "diffusion equation method"[6] which has been fairly successful on a series of demanding problems.[7] The diffusion equation method relies on the treatment of the potential energy hypersurface as an initial concentration gradient. The concentration is propagated forward in time, smoothing the potential surface until there remains only one minimum. The minimum of the smoothed concentration is located and tracked as the diffusion is reversed, running backward in time, to recover the initial, undistorted potential surface. The hope is that the last surviving minimum on the smoothed surface maps back to the global minimum of the potential energy surface. This strategy has worked on a number of n-mers of Lennard-Jones clusters.[7]

Another powerful optimization method is simulated annealing.[8] In the annealing procedure the system is initially equilibrated at a very high temperature at which barriers of the energy hypersurface are easily crossed on the simulation time scale. The temperature is then lowered stepwise at a slow rate with an equilibration period at each new temperature. When the rate of cooling is optimal the annealing procedure is guaranteed to locate the global minimum of the surface. However, as an approach to the protein folding problem, simulated annealing shares the same ailment with the kinetic approach—the required simulation time is far too great. Faster cooling schedules or quenches may be used, but with the cost that there is no guarantee that the minimum found is the optimal one. Another difficulty lies in using the "real" (*ab initio* quantum mechanical) energy function of the protein which, at the high initial temperatures required, allows unwanted changes in conformation (the conversion of L- to D-amino acids, the inversion of chiral centers, and bond breaking and reformation).

There are a number of other global optimization schemes, all of which must deal with two serious problems that are characteristic of protein folding. The first is that the bare potential energy surface as viewed by a classical point particle contains more information than we would like. Many of the potential minima have high energies and are not thermodynamically important. Methods such as the diffusion equation method,[6] as well as the "shift method" of Pillardy, Olszewski, and Piela[9] and the "ant–Lion strategy" of Stillinger and Stillinger,[10] seek to smooth out or "coarse-grain" the potential surface, thus removing the uninteresting minima. In a sense, this is also what is done when distance constraints derived from experimental information such as NMR or X-ray crystallography are imposed, thereby limiting the conformational space accessible to the protein.

A second difficulty afflicting many minimization schemes is their dependence on local information derived from the potential energy surface (the energy and its first and sometimes second derivatives at a single point). Methods proposed recently which address this limitation are the "quasi-quantal method" of Somorjai[11] and the "mean field theory" of Olszewski, Piela, and

† Present address: Department of Chemistry, Wellesley College, Wellesley, MA 02181-8201.

0022-3654/93/2097-6715$04.00/0

Scheraga.[12] In both procedures, an estimate of the ground-state wave function for the time-independent Schrödinger equation is sought. Once obtained, the ground-state wave function may be interpreted as a probability distribution, informing us of the lowest energy regions of the potential surface. An appealing aspect of this class of methods is that favorable minima are sought out by tunneling rather than by the thermally activated barrier crossing required by all classical algorithms.

In this paper we present an optimization algorithm based on the approximate solution of the imaginary time Schrödinger equation via a mobile basis set. The compromises we draw are that our basis for each particle is constrained to have a Gaussian shape and the n-body wave function is constructed as a Hartree product of single-particle wave functions. However, we retain the desirable feature of using nonlocal information about the potential surface to make our moves on the surface, and we can also search out favorable minima through tunneling rather than thermal activation over barriers. That is, whereas methods like quenching and simulated annealing explore only one phase point at a time, the imaginary time algorithm explores extended volumes of configuration space at once, feeling the contour of whole regions of the terrain before flowing to a more favorable region, tunneling through unfavorable regions if need be.

Below, we delineate the central features of the imaginary time algorithm through application to an asymmetric double-well potential. We then find the correct global energy minimum for a series of Lennard-Jones clusters of up to 19 atoms.

II. General Formalism

The imaginary (Euclidean) time form of the time-dependent Schrödinger equation is

$$\frac{\partial}{\partial\tau}\phi(r,\tau) = -H\phi(r,\tau) \tag{1}$$

where the Hamiltonian operator H is defined by

$$H = -\frac{\hbar^2}{2m}\nabla^2 + V(r) \tag{2}$$

Here $\hbar$ is Planck's constant, $V(r)$ is the potential energy, and m is the mass. Note that "time" has units of inverse energy ($\tau \equiv it/\hbar$).

The formal solution of the imaginary time Schrödinger equation is $\phi(r,\tau) = \exp(-H\tau)\phi(r,0)$. Recalling that the equilibrium distribution function is $\exp(-H/k_BT)$, where k_B is the Boltzmann constant and T is the temperature, we see that time plays the role of an inverse temperature. Increasing imaginary time is equivalent to lowering the temperature.

The formal solution for the time evolution of the expectation value $\langle A\rangle$ of an operator A is

$$\langle A\rangle = \frac{\langle\phi(r,0)|e^{-\tau H}Ae^{-\tau H}|\phi(r,0)\rangle}{\langle\phi(r,0)|e^{-2\tau H}|\phi(r,0)\rangle} \tag{3}$$

The general equation for the time dependence of the expectation value of A is found by differentiating eq 3 with respect to τ

$$\frac{d\langle A\rangle}{d\tau} = -\langle HA + AH\rangle + 2\langle A\rangle\langle H\rangle \tag{4}$$

Suppose we knew all the eigenstates of the Hamiltonian H, i.e., all the functions $u_n(r)$ that satisfy the eigenvalue equation $Hu_n(r) = E_nu_n(r)$, where the eigenvalue E_n is the energy of the nth eigenstate u_n. Then the general solution of the imaginary time Schrödinger equation is

$$\phi(r,\tau) = \sum_n a_nu_n(r)\exp(-E_n\tau) \tag{5}$$

Here the sum is over all the eigenstates $u_n(r)$, of which there are typically an infinite number. The only time dependence comes in the exponential factor, from which we see that the contribution to $\phi(r,\tau)$ from the nth eigenstate decays exponentially, relative to the ground (or lowest energy) eigenstate. Thus, after a sufficiently long "time", the only contribution left to $\phi(r,\tau)$ is that from the ground state, provided the initial wave function had a nonzero contribution from the ground state.

The ground state is by definition the optimal configuration. In the limit $\hbar \to 0$ and $\tau \to \infty$, this configuration lies at the bottom of the single deepest potential well, if there is a unique minimum. For nonzero $\hbar$, the relative importance of each minimum is given by the wave density $|\phi(r,\tau \to \infty)|^2$ in that minimum. For computational purposes, one may start with an artificially large value for $\hbar$, which fixes a lower bound on the resolution of conformation space achievable. To achieve greater resolution of the ground-state structure, one simply decreases the value of $\hbar$.[13] A nonzero $\hbar$ may also be considered in terms of setting a nonzero zero-point energy for the system. A large enough zero-point energy will connect all potential minima with each other. This is the lakes-to-oceans transition discussed in other contexts by Simon, Dobrosavljevic, and Stratt.[14]

The use of the imaginary time Schrödinger equation for ground-state searches is not a new idea.[15-17] However, a problem has been the task of choosing a basis set intelligently. Where should we place the elements of the basis set to do the most good? This task is formidable in many-body systems, when the final configuration can be very different from the initial one and when an unintelligent basis set may be enormous. Our contribution to the use of the imaginary time Schrödinger equation for global minimum searches is the use of mobile Gaussian wave packets, first popularized for the real time Schrödinger equation by Heller.[18,19] We derive in the next section equations of motion in imaginary time for the wave packets, which move and adjust themselves to optimize the total energy within the Gaussian constraint.

III. Imaginary Time Equations for Gaussian Wave Packets

We consider first a single particle in d-dimensional space. Extension to the many-body problem is discussed at the end of this section. We take the wave function of each particle to be Gaussian

$$\phi(r,\tau) = (2\pi\sigma^2)^{-d/4}\exp\left[-\left(\frac{r-r_0}{2\sigma}\right)^2\right] \tag{6}$$

We neglect the explicit time dependences of r_0 and σ for notational simplicity.

The equations of motion for the wave packet of each particle are determined by specifying the equations of motion for the packet center, $r_0 = \langle r\rangle$, and its width or second moment $M_2 = \langle(r-r_0)^2\rangle = d\sigma^2$. Direct substitution of r and $(r-r_0)^2$ into eq 4 leads to the equations of motion for the wave packet in imaginary time

$$\dot{r}_0 = -2\langle(r-r_0)V(r)\rangle \tag{7}$$

$$\dot{M}_2 = \frac{d\hbar^2}{2m} - 2[\langle(r-r_0)^2V(r)\rangle - \langle(r-r_0)^2\rangle\langle V(r)\rangle] \tag{8}$$

These equations are identical to those that would result from a Dirac–Frenkel variational approach,[20] adapted to imaginary times. Note that the imaginary time equations depend explicitly on $\hbar$.

For a Gaussian wave packet, the imaginary time equations of motion may be simplified to

$$\dot{r}_0 = -\frac{2}{d}M_2\nabla_{r_0}\langle V\rangle \tag{9}$$

$$\dot{M}_2 = \frac{d\hbar^2}{2m} - \frac{2}{d^2}M_2^2\nabla_{r_0}^2\langle V\rangle$$

We make five observations concerning the properties of these equations.

(1) The equation of motion for the packet center has the form of a steepest descent equation

$$\dot{r}_0 \propto -\nabla_{r_0}\langle V\rangle \tag{10}$$

The packet center moves according to the negative gradient of the effective potential $\langle V\rangle$—that is, the negative gradient of the potential energy averaged over the extent of the wave packet. However, the effective potential depends on time through both r_0 and M_2. We shall see in the application to the double well that the dependence on M_2 brings in a dependence on the kinetic energy, so that the wave packet center appears to move on an effective total energy surface, rather than an effective potential energy surface.

(2) The positive term $d\hbar^2/2m$ acts to expand the wave packet. It plays the role of a diffusion constant in the classical diffusion equation. For the case of a free particle, the imaginary time Schrödinger equation reduces to the diffusion equation, with the solution that the center of the wave packet is fixed while the wave packet squared-width increases linearly in time as

$$M_2(\tau) = \frac{d\hbar^2}{2m}\tau + M_2(0) \tag{11}$$

(3) For the case of the harmonic oscillator, $V(r) = m\omega^2(r - r_m)^2/2$ with effective potential

$$\langle V\rangle = \frac{m\omega^2}{2}[d\sigma^2 + (r_0 - r_m)^2] \tag{12}$$

the equations of motion are

$$\dot{r}_0 = -\frac{2}{d}M_2 m\omega^2(r_0 - r_m) \tag{13}$$

$$\dot{M}_2 = \frac{d\hbar^2}{2m} - \frac{2}{d}M_2^2 m\omega^2$$

and, using the fact that M_2 is independent of r_0, we find

$$M_2(\tau) = \frac{d\hbar}{2m\omega}\tanh(\hbar\omega\tau + a) \tag{14}$$

$$r_0(\tau) = r_m + \frac{b}{\cosh(\hbar\omega\tau)} \tag{15}$$

where a and b are constants determined by the initial values of $r_0(0)$ and $M_2(0)$. Note that the width approaches its optimal value independently of the wave packet center and at a rate that is twice as fast ($\hbar\omega$ for r_0 and $2\hbar\omega$ for the width). Also note that both rates are slower for small $\hbar$.

(4) When the wave packet is sitting in a minimum of the effective potential ($\nabla_{r_0}^2\langle V\rangle > 0$), the effective potential acts to decrease the rate at which the wave packet expands. When the wave packet is sitting on a maximum of the effective potential ($\nabla_{r_0}^2\langle V\rangle < 0$), the effective potential acts to increase the rate at which the wave packet expands.

(5) In many-body systems, the total wave function may be approximated as a Hartree product of the wave functions of the N individual particles

$$\psi(r^N,\tau) = \prod_{k=1}^{N}\phi_k(r_k,\tau) \tag{16}$$

Similarly, the potential energy can be written as a sum over the individual pair interaction energies

$$\langle V\rangle = \sum_{i>j=1}^{N}\int dr_i\int dr_j\,\rho_i(r_i)\,\rho_j(r_j)V(|r_i - r_j|) \tag{17}$$

where $\rho_i(r_i) \equiv \phi_i^*(r_i)\phi_i(r_i)$ and $V(r)$ is averaged over the positions of all the other particles—a mean field potential.[21] Equations 9, 16, and 17 define the equations of motion for the center and width of the wave function for a many-body system.

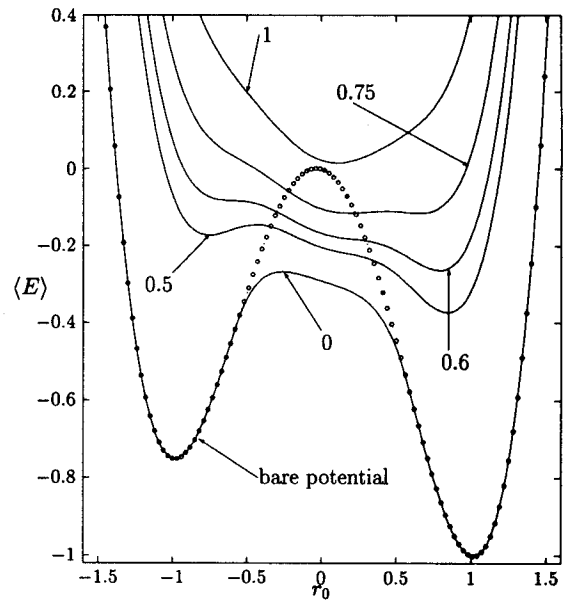

Figure 1. Effective energy for the quartic double-well potential for four values of $\hbar$. For $\hbar = 0.75$ there are two minima (see Figure 3). The effective energy is determined as the sum of the kinetic energy, $d\hbar^2/8mM_2$, and the effective potential, $\langle V(r_0,M_2^{ad})\rangle$, using the adiabatic value of M_2 at each value of r_0.

IV. Applications

In this section we present two applications of the imaginary time algorithm for global minimum searches, the one-dimensional asymmetric quartic double well and Lennard-Jones clusters of up to 19 atoms. We find in both cases that a sufficiently large value of $\hbar$ allows the system to overcome any barrier to the topologically correct global minimum. Reducing $\hbar$ to zero then causes the system to settle into this global minimum.

One might suspect that the value of $\hbar$ is related to a quantum contribution to the kinetic energy that allows the wave packet to *surmount* barriers. However, in the application to the double well, we find that even a small value of $\hbar$ may allow the system to *tunnel through* the barrier.

In our usage, a wave packet is tunneling when its total energy is less than the value of the bare potential at the wave packet center. For example, it is possible for a wave packet whose total energy is less than the energy of a barrier to cross that barrier, under our imaginary time dynamics, provided the wave packet is sufficiently spatially delocalized. This result is true even for zero $\hbar$. However, we find that even a small value of $\hbar$ significantly enhances the propensity of a wave packet to tunnel.

A. Quartic Double-Well Potential. Consider in one dimension the asymmetric quartic double-well potential

$$V(r) = \frac{7}{8}r^4 - \frac{7}{4}r^2 - \frac{1}{8}r \tag{18}$$

With Gaussian wave packets, the effective potential is

$$\langle V\rangle = \frac{7}{8}[r_0^4 + 6M_2r_0^2 + 3M_2^2] - \frac{7}{4}[r_0^2 + M_2] - \frac{1}{8}r_0 \tag{19}$$

The deeper well is the right well. The barrier is at $r_0 = 0$ (see Figure 1).

To simplify the analysis of the imaginary time dynamics, we also consider the following scheme. For any value of r_0, we can imagine integrating to convergence the imaginary time equation of motion for M_2, keeping r_0 fixed. Thus we are finding the optimal value of M_2, for given r_0. We refer to this scheme as the adiabatic version of the imaginary time equations. For general

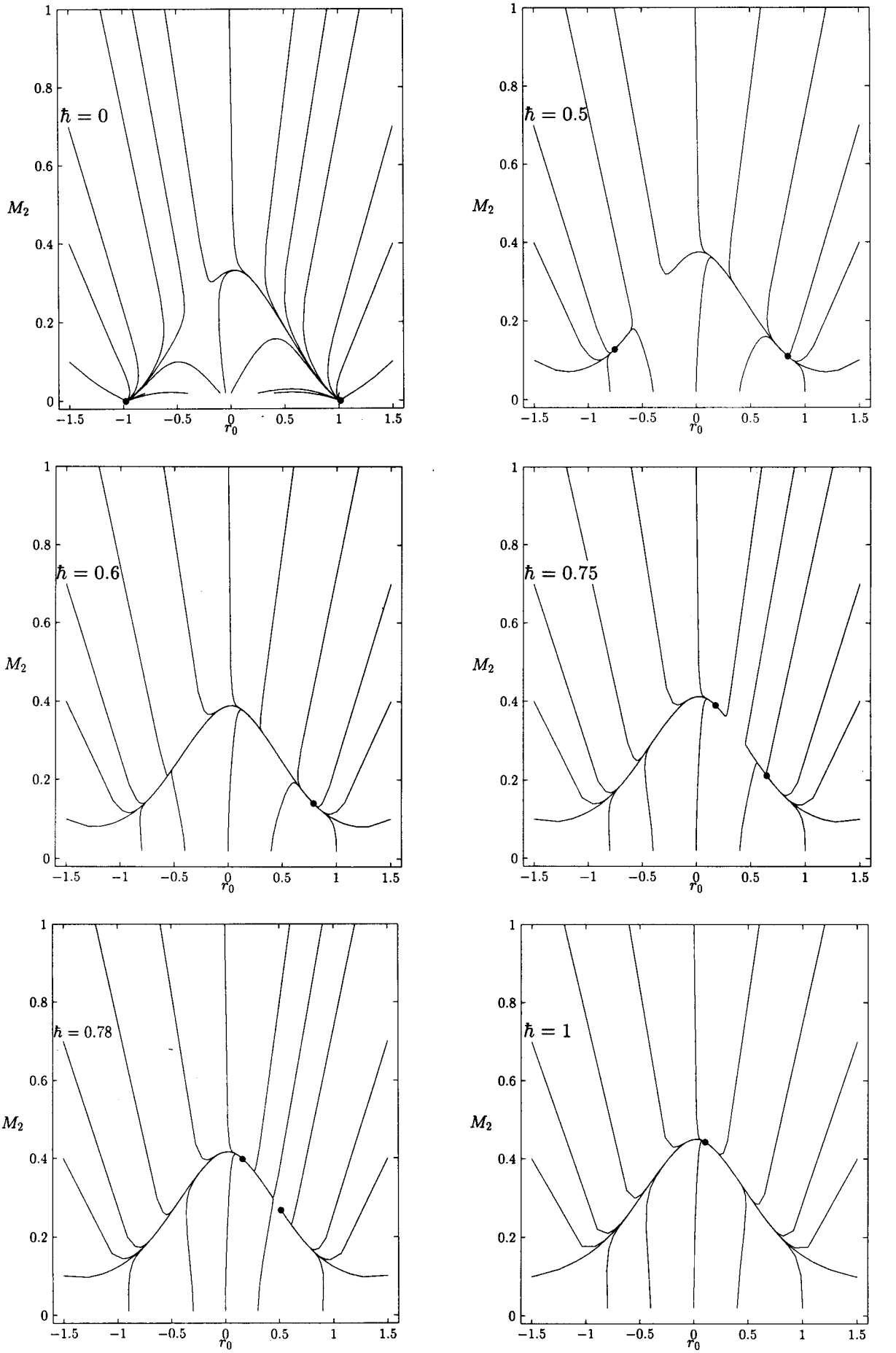

Figure 2. Optimization trajectories for the quartic double-well potential for six values of $\hbar$ representing the four regions of $\hbar$ for which there exist one (regions I and III) or two (regions II and IV) stationary minima.

potentials, this scheme is not practical, but for the quartic potential, the adiabatic M_2 can be found analytically by setting eq 8 equal to zero and solving a cubic equation for the roots. For $\hbar \neq 0$, there is only one real root, which we label M_2^{ad}. For $\hbar = 0$, there is only one nonzero root.

The full imaginary time and the adiabatic equations of motion were integrated using the Bulirsch–Stoer algorithm[22] with a time step of 5×10^{-3} and an internal relative error tolerance of 10^{-8}. For any choice of initial conditions (r_0, M_2) and $\hbar > 0.3$, we find that the full imaginary time scheme value for M_2 converges quickly to the adiabatic value M_2^{ad}, tracking it thereafter as the center attempts to cross the barrier into the deeper well (see Figure 2).

Note that for small $\hbar$, there are two possible values to which r_0 converges, corresponding to trapping of the Gaussian wave packet in either of the two potential wells. Note also that for small values of $\hbar$, the Gaussian wave packet is not likely to tunnel through the barrier unless either the initial r_0 is sufficiently close to the barrier, or the initial M_2 is very large. As $\hbar$ increases, the range of possible initial values of r_0 and M_2 that finds the right potential well increases rapidly. In Figure 3 we show the values to which r_0 converges as a function of $\hbar$. For $\hbar$ larger than about 0.6, all initial wave packets find the correct potential well. (The correct potential well is found if, after converging a trajectory with nonzero $\hbar$, that wave packet sinks to the bottom of the right potential well when $\hbar$ is next set to zero.)

As $\hbar$ further increases, double-valued solutions of r_0 reappear (see region II in Figure 3). Because of the incompleteness of the basis set, two optimal solutions are possible in this region. In one case, the wave packet is resting farther down the potential well, thus minimizing the potential energy at the expense of a higher kinetic energy (narrower wave packet). In the other case, a fatter wave packet (lower kinetic energy) sits higher up in the well. However, either solution is equally good for our purpose since both settle to the bottom of the correct potential well once $\hbar$ is set to zero.

Region II can also be analyzed in terms of the motion of the Gaussian center on an energy surface. The form of the r_0 equation of motion, eq 7, suggests a steepest descent approach on an effective potential surface to the minimum of that potential energy surface. However, r_0 is nonlinearly coupled to M_2, with the result that r_0 appears to move on an effective adiabatic *total* energy surface $E^{ad}(r_0) = \langle H(r_0, M_2^{ad}) \rangle$, or

$$E^{ad}(r_0) = \frac{d\hbar^2}{8mM_2^{ad}} + \langle V(r_0, M_2^{ad}) \rangle \tag{20}$$

We have plotted the effective adiabatic energy $E^{ad}(r_0)$ for a series of $\hbar$ in Figure 1. Notice that for $\hbar = 0.75$, the effective adiabatic energy surface exhibits two shallow wells. In fact, we find that for $\hbar > 0.3$ the dynamics of wave packet relaxation closely follow the full imaginary time algorithm trajectory if we perform a steepest descent calculation on the effective adiabatic total energy surface.

We also point out that increasing $\hbar$ greatly smooths the effective adiabatic energy surface, raising the minima and lowering the barrier. Both effects enhance the ability of the wave packet to tunnel through the barrier. Note that the effective adiabatic energy is *lower* than the barrier height of the bare potential for $\hbar$ in the range 0.6–1.0, and yet the wave packet is able to cross over to the correct side of the barrier regardless of initial conditions.

B. Lennard-Jones *n*-mer Clusters (n = 2–19). For a general potential, $\langle V \rangle$ is conveniently evaluated by fitting the potential to a sum of Gaussian functions. A three-term sum of Gaussians is known to give a very accurate representation of the Lennard-Jones potential for neon.[19] For the case of Gaussian wave packets we need evaluate only the first and second derivatives of the

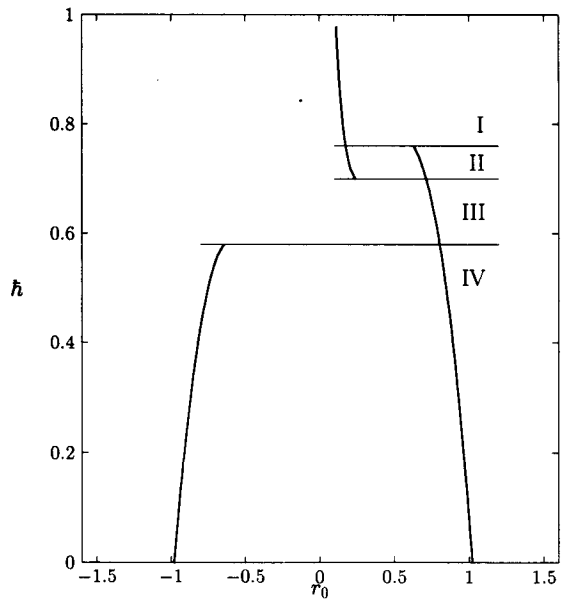

Figure 3. Position of all global minima over a range of possible $\hbar \in [0, 1]$. Four regions of $\hbar$ are indicated for which there exists one (regions I and III) or two (regions II and IV) stationary minima.

effective potential $\langle V \rangle$. For the Gaussian potential, $V(r) = \exp(-\lambda(r - r_m)^2/2)$, one finds

$$\langle V \rangle = \left(\frac{\hat{\lambda}}{\lambda}\right)^{d/2} \exp\left[-\frac{1}{2}\hat{\lambda}(r_0 - r_m)^2\right] \tag{21}$$

$$\nabla_{r_0}\langle V \rangle = -\hat{\lambda}(r_0 - r_m)\langle V \rangle$$

$$\nabla_{r_0}^2\langle V \rangle = \hat{\lambda}[\hat{\lambda}(r_0 - r_m)^2 - d]\langle V \rangle$$

where $\hat{\lambda} = \lambda/(1 + \lambda M_2/d)$. The parameters for the four Gaussian fit to the Lennard-Jones potential used in this work are given in Table I.

Each initial cluster configuration was chosen randomly from an equilibrium liquid configuration of 512 Lennard-Jones atoms. The shortest distance between two particles was 3 Lennard-Jones units, and the largest distance was 12 Lennard-Jones units. Initially, $\hbar$ was chosen in a range from $\hbar = 0$ ($n = 2$ and 3 atoms) to $\hbar = 2$ (larger clusters). The initial value of M_2 was fixed to be 1.0 (see Table II). The equations were first integrated until convergence $\dot{E}/E^2 \leq 10^{-5}$ with nonzero $\hbar$ (see Table II); next the configuration was quenched using the imaginary time equations of motion with $\hbar = 0$ and a convergence criterion $\dot{E}/E^2 \leq 10^{-25}$. Finally, a conjugate gradient algorithm with the *exact Lennard-Jones potential* was used to refine the energy of the minimum found with the imaginary time algorithm. This refinement never exceeded 0.2 Lennard-Jones energy units. The 4th order Runge–Kutta integrator[22] was chosen for its accuracy. All CPU timings were less than 2000 s for all clusters. No special steps were taken to optimize the computer code. For example, tabling the force could lead to a significant saving in computer time.

For large values of $\hbar$, atoms were repelled from one another initially. Therefore, we introduced a harmonic pair potential that prevented the particles from dissociating from the cluster. The confining potential was of the form

$$V_{confine} = \sum_{i>j} \kappa r_{ij}^2/2 \tag{22}$$

where κ was taken from 0.1 (small clusters) to 0.03 (larger clusters) and r_{ij} is the distance between the packet centers for the ith and jth particles (see Table II).

Near convergence to the ground state, the energy should decay exponentially, with a rate given by the energy difference between the first excited state and the ground state (see section II).

TABLE I: Parameters for the Gaussian Decomposition of the Lennard-Jones Potential of the Form $V(r) = \sum_k a_k e^{-b_k r^2/2}$ Given in Lennard-Jones Reduced Units

a_k	b_k	a_k	b_k
846 706.7	30.928 81	−0.715 442 0	1.279 242
2713.651	14.693 75	−9.699 172	3.700 745

TABLE II: Summary of Results for the Global Energy Optimization for Lennard-Jones Atomic Clusters. The Initial Value of $M_2(0) = 1.0$. Energies Are Given in Lennard-Jones Reduced Units

no. of atoms	no. of minima[7]	global minimum[24]	imaginary time	$\hbar$	κ	DEM[7]
2	1	−1.000	−1.000	0.0	0.0	global
3	1	−3.000	−3.000	0.0	0.0	global
4	1	−6.000	−6.000	0.0	0.1	global
5	2	−9.104	−9.104	0.0	0.1	global
6	2	−12.712	−12.712	0.4	0.1	global
7	4	−16.505	−16.505	0.4	0.1	global
8	8	−19.822	−19.821	0.5	0.05	local
9	18	−24.113	−24.113	0.5	0.1	local
10	57	−28.420	−28.422	0.5	0.1	local
11	145	−32.765	−32.7659	1.5	0.05	global
12	366	−37.967	−37.9676	1.5	0.05	local
13	988	−44.327	−44.327	1.5	0.05	global
14	~3258	−47.845	−47.845	1.5	0.04	global
15	~10700	−52.322	−52.3226	2.0	0.04	global
19	~2 × 10^6	−72.659	−72.6598	2.0	0.03	local

Assuming that this is true for the imaginary time algorithm, at every third time step we analytically fit the energies from the two previous time steps to an exponential decay, $E(\tau) \propto A + B \exp(-\gamma\tau)$. An estimate of the new time step was determined by setting the relative change in the energy equal to a constant:

$$\gamma\delta\tau = \delta\tau\left|\frac{\ddot{E}}{\dot{E}}\right| = 2\left|\frac{E(\tau+\delta\tau) - 2E(\tau) + E(\tau-\delta\tau)}{E(\tau+\delta\tau) - E(\tau-\delta\tau)}\right| = \lambda \quad (23)$$

where λ is a constant. We use $\lambda = 1.6$. At the end of each trajectory, with the imaginary time equations nearly converged, the time step which satisfies the above criterion became as large as 10^{30}. Apparently, a too rapid increase in the time step can lead to inaccuracy in the integration of the equations of motion. For the $n = 15$ cluster we found it necessary to determine a new time step with $\lambda = 0.35$.

For Lennard-Jones clusters as large as 19 atoms, we were consistently able to find the global minimum of the cluster. The results are presented in Table II and compared with the results of the diffusion equation method.[7] In Figure 4 we display the global minimum geometries for the 13-atom cluster where both the diffusion equation method and our imaginary time algorithm find the correct global minimum. We also present the global minimum structure for the 12- and 19-atom clusters where the imaginary time algorithm converges to the correct minima (the Mackay icosahedron with a surface atom removed and the double icosahedron, respectively). For a 12-atom cluster, the diffusion equation method converges to a low lying local minimum of an icosahedron with the central atom removed.[7]

In Figure 5 we plot the displacement of each atom from its position in the global minimum configuration as a function of imaginary time. For both the 7- and 13-atom clusters, it is possible to identify single and multiple particle rearrangements as the cluster relaxes to its minimum energy configuration. For the case of the 13-atom cluster, there is rapid convergence to an expanded icosahedron where one atom has moved to the center of the cluster and all other atoms are approximately 1.6 σ from the minimum energy configuration. This large value reflects the enlarged steady-state width of the wave packet at higher $\hbar$. When $\hbar$ is reduced to zero, the expanded icosahedron contracts to the correct scale for wave packets of zero width.

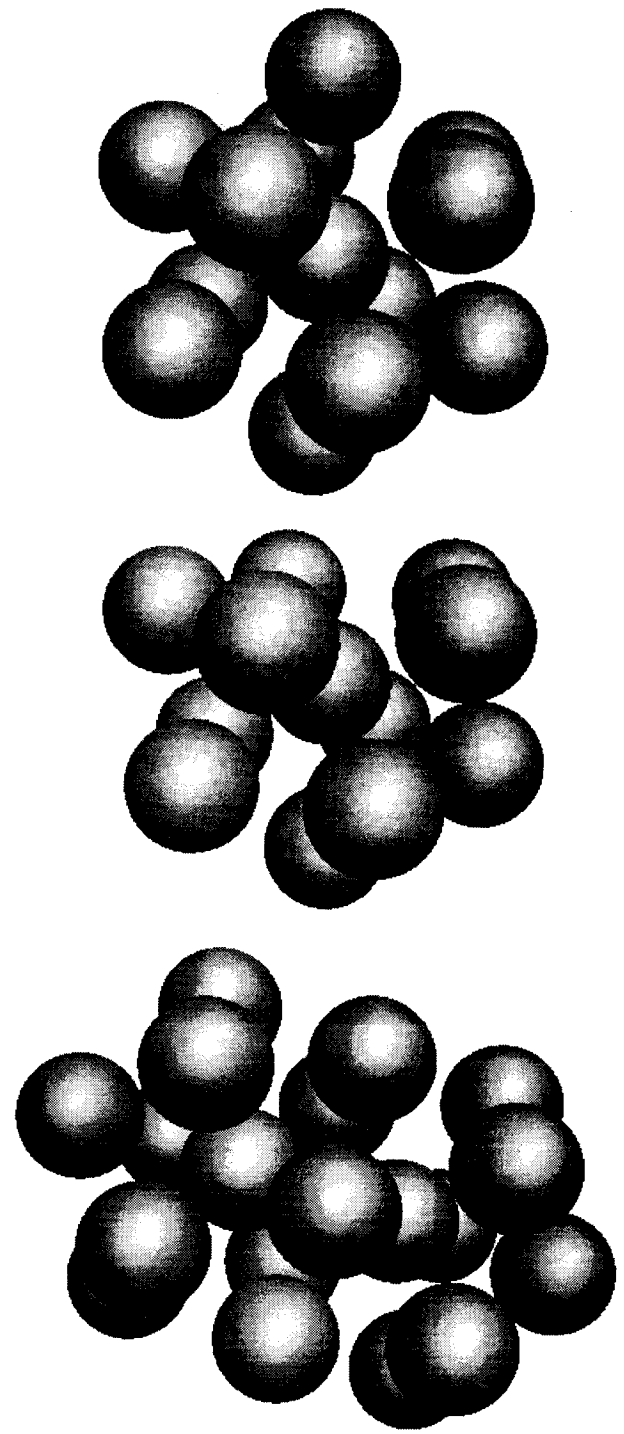

Figure 4. Global minimum configurations for Lennard-Jones n-mer clusters (a, top) $n = 13$ (Mackay icosahedron), (b, middle) $n = 12$ (icosahedron with one surface atom removed), and (c, bottom) $n = 19$ (double icosahedron).

V. Conclusion

We have presented a deterministic algorithm for energy minimization of classical many-body systems based on an approximate solution of the imaginary time Schrödinger equation using Gaussian wave packets. We have discussed the similarity of our method to the "diffusion equation method" of Piela, Kostrowicki, and Scheraga.[6] The imaginary time algorithm found with a modest effort the global minimum of Lennard-Jones clusters containing as many as 19 atoms. This is a somewhat better record than that of the diffusion equation method for clusters with 19 atoms or less. However, we note that the diffusion equation method has been tested for a 55-atom cluster where it located the global energy minimum. In closing we discuss at greater length

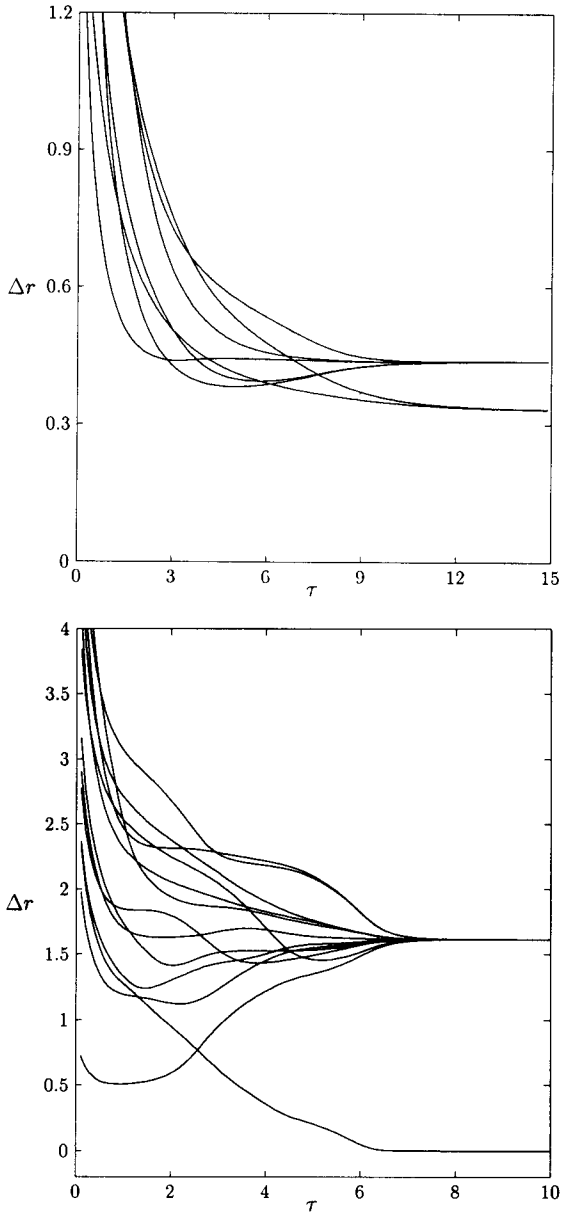

Figure 5. Displacement of each atom from its position in the global minimum configuration $\Delta r = |r - r_{min}|$ is shown as a function of imaginary time for two clusters (a, top) $n = 7$ and (b, bottom) $n = 13$ (Mackay icosahedron).

the similarity of the imaginary time method to the diffusion equation method (hereafter DEM).

The deformed interaction potential employed in DEM (see eq 10 in ref 7) is identical to the effective potential defined in eq 21, if the mean squared-width of the Gaussian wave packet M_2 is identified with the diffusion "time" of DEM. In DEM, this "time" is the same for all the particles, which in the imaginary time method corresponds to having the same Gaussian width for each particle. In DEM, the initial conditions are chosen to correspond to an optimal diffusion time where there are few or, as is the case for Lennard-Jones clusters, one surviving minimum. The diffusion time is then gradually reduced toward zero; in the imaginary time method, this corresponds to decreasing the width of each Gaussian wave packet. In DEM, at each new time or value of M_2, the energy minimum is found by steepest descent before taking another time step.[23]

Similarly, in the imaginary time algorithm we initially choose large M_2 values. However, in the imaginary time algorithm, the value of M_2 is not constrained to be the same for every particle. Moreover, M_2 is not constrained to decrease monotonically. The entire dynamics of all the individual Gaussian centers r_0 and widths M_2 varies for each particle such as to optimize the total energy.

Thus DEM may be viewed as a special case of the imaginary time algorithm where (1) $\hbar = 0$, (2) the wave packets all have the same squared-width M_2, and (3) the magnitude of M_2 is initially set to something large and then monotonically decreased to zero. The greater flexibility of the imaginary time algorithm and the fact that the equations of motion are variationally based may help to explain the greater success of the imaginary time algorithm for the clusters examined in this work.

Acknowledgment. We thank David Coker and Jianpeng Ma for helpful discussions. This work was supported in part by a grant from the Petroleum Research Fund. D.H. thanks David Coker for support.

References and Notes

(1) Stillinger, F. H.; Weber, T. A. *Phys. Rev. A* **1982**, *25*, 978; **1983**, *28*, 2408; *Science* **1984**, *225*, 983.
(2) Frauenfelder, H.; Sligar, S. G.; Wolynes, P. G. *Science* **1991**, *254*, 1598. Frauenfelder, H.; Parak, F.; Young, R. D. *Annu. Rev. Biophys. Chem.* **1988**, *17*, 451.
(3) Hoare, M. R.; McInnes, J. *Faraday Discuss. Chem. Soc.* **1976**, *61*, 12.
(4) Zwanzig, R. *J. Chem. Phys.* **1983**, *79*, 4507.
(5) Gibson, K. D.; Scheraga, H. A. In *Structure and Expression: From Proteins to Ribosomes*; Sarma, M. H., Sarma, R. H., Eds.; Adenine Press: Schenectady, NY, 1988; Vol. 1.
(6) Piela, L.; Kostrowicki, J.; Scheraga, H. A. *J. Phys. Chem.* **1989**, *93*, 3339.
(7) Kostrowicki, J.; Piela, L.; Cherayil, B. J.; Scheraga, H. A. *J. Phys. Chem.* **1991**, *95*, 4113.
(8) Kirkpatrick, S.; Gelatt, C. D., Jr.; Vecchi, M. P. *Science* **1983**, *220*, 671.
(9) Pillardy, J.; Olszewski, K. A.; Piela, L. *J. Phys. Chem.* **1992**, *96*, 4337.
(10) Stillinger, F. H.; Stillinger, D. K. *J. Chem. Phys.* **1990**, *93*, 4266.
(11) Somorjai, R. *J. Phys. Chem.* **1991**, *95*, 4141, 4147.
(12) Olszewski, K. A.; Piela, L.; Scheraga, H. A. *J. Phys. Chem.* **1992**, *96*, 4672; **1993**, *97*, 260, 267.
(13) One may not wish to decrease $\hbar$ beyond its physical value since if the wave packet is not localized in a single well all the contributing wells may be important.
(14) Simon, S. H.; Dobrosavljevic, V.; Stratt, R. M. *J. Chem. Phys.* **1991**, *94*, 7360. The lakes-to-oceans analogy appears in a purely classical context: Zallen, R.; Scher, H. *Phys. Rev. B* **1971**, *4*, 4471.
(15) Anderson, J. B. *J. Chem. Phys.* **1975**, *63*, 1499; **1976**, *65*, 4121; *Int. J. Quantum Chem.* **1979**, *15*, 109.
(16) Feit, M. D.; Fleck, J. A., Jr.; Steiger, A. *J. Comput. Phys.* **1982**, *47*, 412. Feit, M. D.; Fleck, J. A., Jr. *J. Chem. Phys.* **1983**, *78*, 301.
(17) Kosloff, R. *J. Phys. Chem.* **1988**, *92*, 2087.
(18) Heller, E. J. *J. Chem. Phys.* **1975**, *62*, 1544. Heller, E. J. *Acc. Chem. Res.* **1981**, *14*, 368. See also: Gerber, R. B.; Ratner, M. A. *Adv. Chem. Phys.* **1988**, *70*, 97.
(19) In the respect that our goal is to simulate many-body systems, our work is related to the work of Corbin and Singer and Singer and Smith: Corbin, N.; Singer, K. *Mol. Phys.* **1982**, *46*, 671 and Singer, K.; Smith, W. *Mol. Phys.* **1986**, *57*, 761, who apply Gaussian wave packets to the quantum simulation of neon atoms in real time.
(20) Frenkel, J. *Wave Mechanics: Advanced General Theory*; Clarendon Press: Oxford, 1934. In the Dover edition (1950), see p 253, Frenkel cites an appendix in the Russian edition of Dirac's *Principles of Quantum Mechanics*, 1930.
(21) McLachlan, A. D. *Mol. Phys.* **1964**, *8*, 39.
(22) Press, W. H.; Teukolsky, S. A.; Flannery, B. P.; Vetterling, W. T. *Numerical recipes: The art of scientific computing*; Cambridge University Press: Cambridge, 1986.
(23) Related to this work and to the diffusion equation method is a method of global optimization based on the classical density distribution expanded in Gaussians by Shalloway: Shalloway, D. In *Recent advances in global optimization*; Floudas, A., Pardalos, P. M., Eds.; Princeton University Press: Princeton, 1992; p 433.
(24) Hoare, M. R.; Pal, P. *Adv. Phys.* **1971**, *20*, 161.